

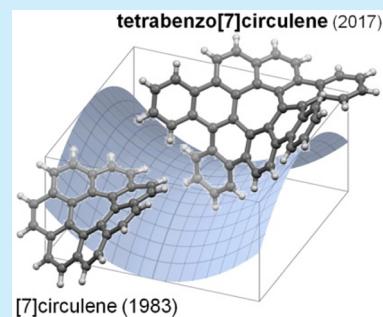
Synthesis, Structure, and Properties of Tetrabenzo[7]circulene

Xiao Gu, Huiyan Li, Bowen Shan, Zhifeng Liu, and Qian Miao*[✉]

Department of Chemistry, The Chinese University of Hong Kong, Shatin, New Territories, Hong Kong, China

Supporting Information

ABSTRACT: Tetrabenzo[7]circulene, a new member of aromatic saddles, was conveniently synthesized from 2-(1-naphthoyl)benzoic acid with the seven-membered ring constructed at an early stage of the synthesis. This method, upon minor modification, was also useful for synthesis of thiophene-annulated [7]circulenes. The structures of tetrabenzo[7]circulene and [7]circulene were compared in terms of symmetry, flexibility, and curvature on the basis of DFT calculations and X-ray crystallography. It was also found that tetrabenzo[7]circulene functioned as a p-type semiconductor in thin-film transistors and cocrystallized with C₆₀.



[7]Circulene (Figure 1)^{1–3} is a member of the [*n*]circulene family, which has a central *n*-membered ring surrounded with *n*-fused benzenoid rings.⁴ The shape of [*n*]circulenes varies depending on the value of *n* as demonstrated by [5]-, [6]-, and [7]circulenes, which have a shape of bowl, flat disk, and saddle, respectively. [7]Circulene is not only the first member of heptagon-embedded nonplanar polycyclic arenes^{5–7} but also can be considered as a basic segment or a model compound for negatively curved nanostructures of sp² carbon,⁸ such as toroidal carbon nanotubes^{9,10} and schwarzites.^{11,12} Moreover, [7]-circulene can, in principle, serve as a synthetic precursor for these interesting but still elusive carbon nanomaterials. Benzannulation is a commonly used strategy to expand and stabilize [*n*]circulenes leading to tetrabenzo[4]circulene,¹³ dibenzo[5]circulene,¹⁴ hexa-peri-hexabenzocoronene^{15,16} hexacata-hexabenzocoronene,¹⁷ and tetrabenzo[8]circulene.^{18,19} However, benzannulated [7]circulenes remained unknown in the literature.²⁰ Here, we report tetrabenzo[7]circulene (**1** in Figure 1) as a new member of polycyclic aromatic saddles, detailing its synthesis, structure, and properties.

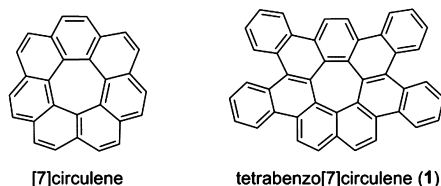
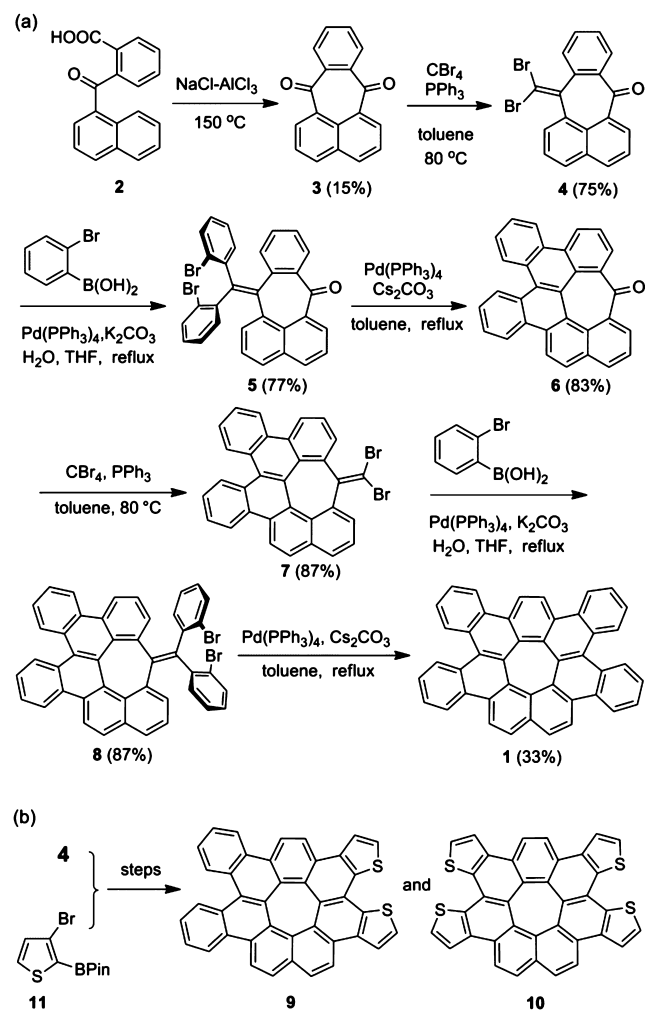


Figure 1. [7]Circulene and tetrabenzo[7]circulene (**1**).

Unlike Yamamoto's syntheses of [7]circulene involving formation of the central seven-membered ring at a late stage,^{1–3} our synthesis of **1** started with formation of the seven-membered ring as shown in Scheme 1. Intramolecular Friedel–Crafts acylation of 2-(1-naphthoyl)benzoic acid (**2**)²¹ in melted NaCl–AlCl₃ led to 5,12-pleiadenedione (**3**), which was

separated from the undesired major product, benz[*a*]anthracene-7,12-dione, with a low yield (15%). In order to expand the polycyclic framework, dione **3** was then subjected to the Ramirez reaction²² and the subsequent Suzuki coupling, which were reported for synthesis of curved polycyclic arenes.^{7,23} Treatment of **3** with 3 equiv of CBr₄ and 6 equiv of PPh₃ yielded compound **4** with only one of the carbonyl groups reacted. To our surprise, even a larger excess of CBr₄ (8 equiv) and PPh₃ (16 equiv) was not able to enforce the reaction of the second carbonyl group, likely because the carbonyl group in **4** is blocked by the bromine atoms on the convex face as found from the crystal structure of **4** (Figure S1, Supporting Information). The Suzuki coupling of **4** with 2-bromophenylboronic acid resulted in **5** with a good yield. The ¹H NMR spectra of **5** showed broad peaks in the aromatic region likely because the rotation of the brominated phenyl rings is restricted by steric hindrance. Pd-catalyzed cyclization of **5** with Pd(PPh₃)₄ as the catalyst and Cs₂CO₃ as the base led to **6** with a yield of 83%. In contrast, cyclized products with formation of five-membered rings via bond formation between the two brominated rings were not isolated from this reaction. Unlike **4**, ketone **6** appeared reactive toward CBr₄ and PPh₃ likely because of the reduced steric hindrance, resulting in **7**, which underwent the second Suzuki coupling to yield **8**. Pd-catalyzed cyclization of **8** under the same conditions for the reaction of **5** yielded **1** as yellow solids. On the other hand, our attempts to synthesize **1** using the Scholl reaction were unfruitful. Treatment of 12-(diphenylmethylene)pleiaden-5-one with DDQ/CH₃SO₃H or FeCl₃ did not yield **6** but led to recovery of starting materials, while treatment of the same compound with DDQ/CF₃SO₃H resulted in a complicated mixture, from which **6** was not isolated. The above route can be modified for synthesis of structurally related molecules. To demonstrate this, we synthesized thiophene-annulated [7]-

Received: March 11, 2017

Scheme 1. (a) Synthesis of **1**; (b) Simplified Synthesis of **9** and **10**

circulenes **9** and **10** (Scheme 1b) by replacing 2-bromophenylboronic acid with 3-bromothiophene-2-boronic acid pinacol ester (**11**) once or twice in the above synthesis, respectively, as detailed in the Supporting Information. In particular, the synthesis of **9**, a desymmetrized molecule, took advantage of **4** with dibromovinylene on only one side.

One interesting aspect of **1** is its stereochemistry in comparison with that of [7]circulene. As found from a recently reported study based on density functional theory (DFT) calculations, [7]circulene can adopt C₂- and C_s-symmetric structures, which are both ca. 9 kcal/mol lower in energy than a planar structure with D_{7h} symmetry.²⁴ In contrast to the reported result,²⁴ the chiral C₂ conformer is found to be slightly less stable than the achiral C_s conformer by 0.11 kcal/mol of Gibbs free energy as calculated at the B3LYP/6-31G(d,p) level of DFT in this study. [7]Circulene exists in crystals as a pair of enantiomers (*P*- and *M*-form) and has a crystallographic 2-fold symmetry with a C₂ axis of symmetry as shown in Figure 2a.² In contrast, the C_s-[7]circulene has not been experimentally observed, and its DFT-calculated model is shown in Figure 2b with the symmetry plane σ. As found from another computational study, [7]circulene is remarkably floppy and can flip via the D_{7h}-symmetric transition state with an energy barrier of 8.5 kcal/mol.²⁵

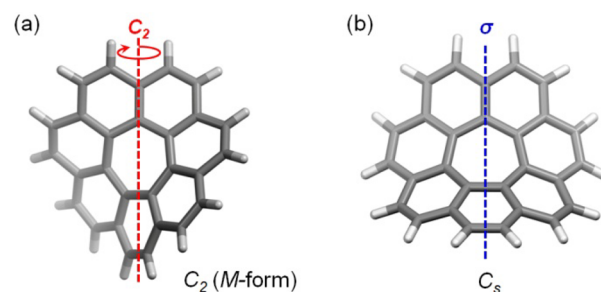


Figure 2. (a) *M*-enantiomer of C₂-[7]circulene in crystals with the C₂ symmetry axis.² (b) Molecular model of C_s-[7]circulene with the symmetry plane as calculated at the B3LYP/6-31G(d,p) level of DFT.²⁵

With four extra benzene rings, molecule **1** has two [4]helicene moieties in addition to the [7]circulene moiety. The structure of **1** was studied with DFT calculations²⁶ and X-ray crystallography. Molecular geometry optimization at the B3LYP/6-31G(d,p) level of DFT reveals saddle-shaped structures of C₂ and C_s symmetry for molecule **1** similar to those for [7]circulene. The C₂-symmetric structure of **1** is chiral, and the two enantiomers of C₂-symmetry can be noted as (*P,M,P*)-**1** and (*M,P,M*)-**1**, where the first and third helicity notation (*P* or *M*) refer to the [4]helicene moieties while the second helicity notation refers to the [7]circulene moiety. In contrast, C_s-**1** is achiral, having its [7]circulene moiety of C_s symmetry and its two [4]helicene moieties of opposite helicities. Figure 3a shows the geometry-

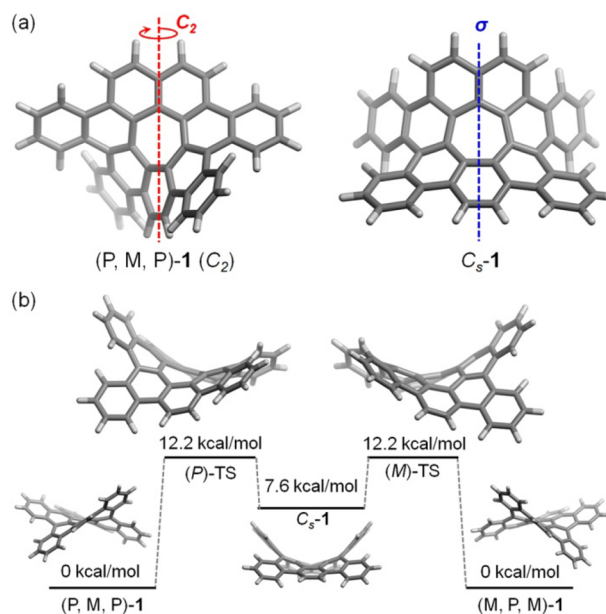


Figure 3. (a) Molecular models of (*P,M,P*)-**1** and C_s-**1**. (b) Structures and relative Gibbs free energy of the intermediates and transition states for the interconversion between (*P,M,P*)-**1** and (*M,P,M*)-**1** as calculated at the B3LYP/6-31G(d,p) level of DFT.

optimized models of (*P,M,P*)-**1** and C_s-**1** with the C₂ axis of symmetry and the symmetry plane σ, respectively. The C₂-symmetric enantiomers (*P,M,P*)-**1** and (*M,P,M*)-**1** are calculated to be more stable than C_s-**1** by 7.6 kcal/mol, which corresponds to an equilibrium constant of 3.7 × 10⁵ at 25 °C for the C_s-to-C₂ isomerization. It is further found that (*P,M,P*)-**1** converts to C_s-**1** through the transition state (*P*)-TS and (*M,P,M*)-**1** converts to C_s-**1** through the transition state (*M*)-TS as shown in Figure 3b. The

two transition-state structures, (*P*)- and (*M*)-TS, are a pair of enantiomers with the same energy barrier (12.2 kcal/mol), which corresponds to a rate constant of $7.1 \times 10^3 \text{ s}^{-1}$ at 25 °C, as estimated using the Eyring equation $k = \kappa(k_B T/h) \exp(-\Delta G^\ddagger/RT)$ and assuming a value of unity for the transmission coefficient (κ).²⁷ Combining the two conversions leads to the calculated pathway for interconversion between (*P,M,P*)-**1** and (*M,P,M*)-**1** as shown in Figure 3b, where *C_s*-**1** is an intermediate. This pathway is though pseudorotation²⁸ with an energy barrier of 12.2 kcal/mol and does not involve planarization of the [7]circulene moiety. The above calculation indicates that (*P,M,P*)-**1** and (*M,P,M*)-**1** are the dominating conformers of **1** with fast interconversion at room temperature.

Sublimation of **1** with a flow of nitrogen gas in a physical vapor transport system²⁹ afforded yellow needle-like crystals suitable for X-ray crystallography. The crystal of **1** is found to contain a pair of enantiomers that are shaped as a twisted saddle (Figure 4a). The structure of **1** in the crystal is very similar to the

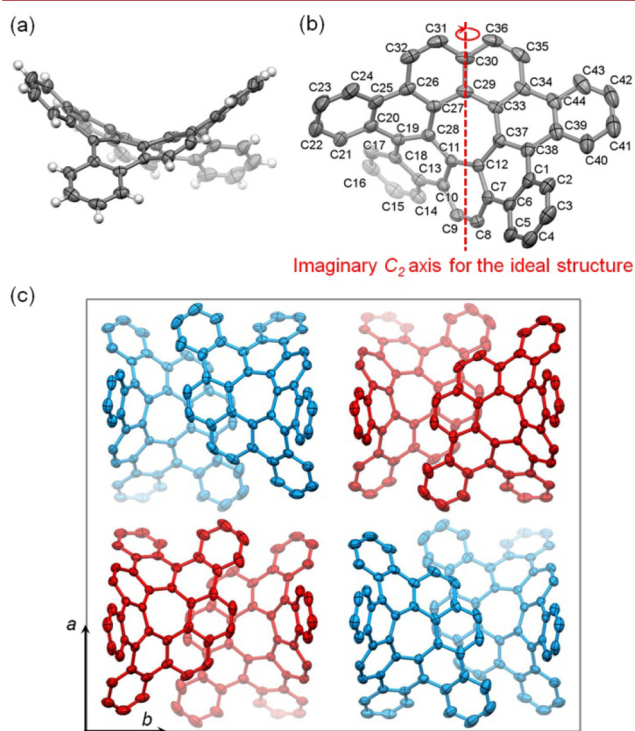


Figure 4. Crystal structure of **1**: (a) side view of (*P,M,P*)-**1** showing the shape of twisted saddle; (b) top-view of (*P,M,P*)-**1** with the labels for carbon atoms and the *C*₂-axis for the ideal structure; (c) unit cell of **1** as viewed along the *c* axis. (Carbon atoms are shown as ellipsoids at 50% probability level, in (b) and (c) H atoms are removed for clarification, in (c) (*P,M,P*)-**1** and (*M,P,M*)-**1** are shown in red and blue, respectively.)

calculated *C*₂-symmetry structure as shown in Figure 4b, but unlike [7]circulene, it lacks a crystallographic 2-fold symmetry. The C–C bonds that are related by the imaginary *C*₂-axis (Figure 4b) only slightly differ in length, and most of these differences in bond length are within the experimental errors. For example, the C30–C31 and C30–C36 bonds are 1.409(5) and 1.406(4) Å long, respectively, and the C31–C32 and C35–C36 bonds are 1.334(5) and 1.330(5) Å long, respectively (the labels for carbon atoms are shown in Figure 4b). Figure 4c shows a unit cell of the crystal of **1** consisting of segregated stacks of (*P,M,P*)-**1** and (*M,P,M*)-**1** (shown in red and blue, respectively), as viewed along the *c* axis. In each stack, molecules of the same handedness stack

with each other having about two benzenoid rings overlapped in a roughly face-to-face manner with intermolecular contacts between carbon atoms as short as 3.37 Å. However, the overlapped benzenoid rings are not exactly parallel with each other because of the curved nature. The crystal structure of **1** also allows us to compare the [7]circulene moiety of **1** and [7]circulene in terms of the depth of the saddle, which can be defined as the distance from C25 or C44 to the plane defined by C11, C12, and C29 in **1**. As shown in Figure S2, it is found that the [7]circulene moiety in **1** is more curved with a depth of saddle of 2.507 Å as measured from C25 or 2.106 Å as measured from C44, while [7]circulene is less curved with a depth of saddle of 1.703 Å as measured from the corresponding carbon atoms. The greater curvature of **1** is presumably because of the additional crowdedness introduced by its two [4]helicene moieties.

Compound **1** forms yellow solutions in CH₂Cl₂ with green fluorescence when irradiated with UV light. As shown in Figure S3, the longest wavelength absorption maxima appears at 413 nm, which shifts to red by about 80 nm relative to that of [7]circulene (326 nm¹ or 331 nm²) in agreement with the expanded π -system of **1**. The emission spectrum of **1** (Figure S3) shows a broad peak at about 520 nm with a large Stokes shift, which is attributable to the flexible framework of **1** since the conformational change shown in Figure 3b can consume the energy of the excited state. The cyclic voltammogram of **1** exhibited one quasi-reversible oxidation wave with a half-wave potential of 0.59 V versus ferrocenium/ferrocene but did not exhibit any reduction waves in the testing window as shown in Figure S4 in the Supporting Information. Based on this oxidation potential, the highest occupied molecular orbital (HOMO) energy level of **1** is estimated as -5.69 eV .³⁰ For comparison, the HOMO and lowest unoccupied molecular orbital (LUMO) energy levels of (*P,M,P*)-**1** are calculated as -5.30 and -2.12 eV at the B3LYP level of DFT with the 6-311++G(d,p) basis set.

The molecular packing and the HOMO energy level of **1** suggest that it can, in principle, function as a p-type semiconductor in the solid state. Thin films of **1** were deposited by thermal evaporation under high vacuum onto a silicon substrate, which had successive layers of silica, alumina, and 12-cyclohexyldodecylphosphonic acid (CDPA) as a composite dielectric material.³¹ Here, CDPA formed a self-assembled monolayer (SAM) on alumina to provide an ordered dielectric surface with a relatively high surface energy.³² The device fabrication was completed by depositing a layer of gold onto the film of **1** through a shadow mask to form top-contact source and drain electrodes. As measured in ambient air, **1** functioned as a p-type semiconductor with a field effect mobility of $5 \times 10^{-4} \text{ cm}^2/(\text{V s})$. This low field effect mobility may be attributed to the amorphous nature of the film, which was found from the absence of diffraction peaks when the film was investigated with X-ray diffraction (XRD).

The intrinsically curved polycyclic framework of **1** suggests that it may cocrystallize with fullerenes because of the complementary shapes. Due to the p-type semiconductor property of **1**, the cocrystals of **1** and fullerenes (n-type semiconductors) may find applications in organic solar cells as a molecular-level p–n heterojunction, which was demonstrated by Nuckolls et al. with nonplanar donor π -molecules and fullerenes.^{33,34} With this consideration, we found that cooling a solution of **1** and C₆₀ in *o*-dichlorobenzene led to cocrystallization of **1** and C₆₀. X-ray crystallography of the resulting black crystals revealed a unit cell containing **1** and C₆₀ in a ratio of 1:1

as well as solvent molecules. However, this crystal structure has an *R* factor as large as 21% due to the disordered orientation of C₆₀ molecules. Such a large *R* factor does not allow us to analyze molecular packing in the cocrystal with high accuracy. Further studies on characterization and application of the cocrystals of **1** and C₆₀ are in progress in our laboratory.

In summary, we developed a convenient synthesis of tetrabenzo[7]circulene (**1**) which, upon minor modification, was also useful for synthesis of thiophene-annulated [7]-circulenes. DFT calculation indicates that the most stable conformers of **1** are two enantiomers of the C₂ symmetry, which interconvert fast at room temperature. In agreement with the calculation, **1** exists in the crystal as two enantiomers having a twisted-saddle shape close to the C₂ symmetry. X-ray crystallography also reveals that the [7]circulene moiety in **1** is more curved than [7]circulene itself. It is found that **1** functions as a p-type semiconductor in thin-film transistors and is able to cocrystallize with C₆₀, an n-type semiconductor.

■ ASSOCIATED CONTENT

Supporting Information

The Supporting Information is available free of charge on the ACS Publications website at DOI: 10.1021/acs.orglett.7b00714.

Details of synthesis and characterization; crystallographic data for **1** and **4**; fabrication and characterization of organic thin film transistors; NMR spectra (PDF)
X-ray data for compound **1** (CIF)
X-ray data for compound **4** (CIF)

■ AUTHOR INFORMATION

Corresponding Author

*E-mail: miaoqian@cuhk.edu.hk.

ORCID

Qian Miao: 0000-0001-9933-6548

Notes

The authors declare no competing financial interest.

■ ACKNOWLEDGMENTS

We thank Ms. Hoi Shan Chan (The Chinese University of Hong Kong) for the single-crystal crystallography. This work was supported by the Research Grants Council of Hong Kong (CRF C4030-14G) and The Chinese University of Hong Kong (Faculty of Science Strategic Development Scheme and the One-Off Funding for Research from Research Committee).

■ REFERENCES

- (1) Yamamoto, K.; Harada, T.; Nakazaki, M.; Naka, T.; Kai, Y.; Harada, S.; Kasai, N. *J. Am. Chem. Soc.* **1983**, *105*, 7171.
- (2) Yamamoto, K.; Harada, T.; Okamoto, Y.; Chikamatsu, H.; Nakazaki, M.; Kai, Y.; Nakao, T.; Tanaka, M.; Harada, S.; Kasai, N. *J. Am. Chem. Soc.* **1988**, *110*, 3578.
- (3) Yamamoto, K.; Sonobe, H.; Matsubara, H.; Sato, M.; Okamoto, S.; Kitaura, K. *Angew. Chem., Int. Ed. Engl.* **1996**, *35*, 69.
- (4) Feng, C.-N.; Kuo, M.-Y.; Wu, Y.-T. *Angew. Chem., Int. Ed.* **2013**, *52*, 7791.
- (5) (a) Yamamoto, K. *Pure Appl. Chem.* **1993**, *65*, 157. (b) Kawasumi, K.; Zhang, Q.; Segawa, Y.; Scott, L. T.; Itami, K. *Nat. Chem.* **2013**, *5*, 739. (c) Pradhan, A.; Dechambenoit, P.; Bock, H.; Durola, F. *J. Org. Chem.* **2013**, *78*, 2266. (d) Márquez, I. R.; Fuentes, N.; Cruz, C. M.; Puente-Muñoz, V.; Sotorrios, L.; Marcos, M. L.; Choquesillo-Lazarte, D.; Biel, B.; Crovetto, L.; Gómez-Bengoia, E.; González, M. T.; Martín, R.; Cuerva, J. M.; Campaña, A. G. *Chem. Sci.* **2017**, *8*, 1068.

- (6) (a) Luo, J.; Xu, X.; Mao, R.; Miao, Q. *J. Am. Chem. Soc.* **2012**, *134*, 13796. (b) Mughal, E. U.; Kuck, D. *Chem. Commun.* **2012**, *48*, 8880. (c) Ip, H.-W.; Ng, C.-F.; Chow, H.-F.; Kuck, D. *J. Am. Chem. Soc.* **2016**, *138*, 13778.
- (7) Cheung, K. Y.; Xu, X.; Miao, Q. *J. Am. Chem. Soc.* **2015**, *137*, 3910.
- (8) Cheung, K. Y.; Miao, Q. In *Polycyclic Arenes and Heteroarenes: Synthesis, Properties and Applications*; Miao, Q., Ed.; Wiley VCH: Weinheim, 2016; Chapter 1, p 85.
- (9) Chuang, C.; Fan, Y.-C.; Jin, B.-Y. *J. Chem. Inf. Model.* **2009**, *49*, 361.
- (10) Beuerle, F.; Herrmann, C.; Whalley, A. C.; Valente, C.; Gamburd, A.; Ratner, M. A.; Stoddart, J. F. *Chem. - Eur. J.* **2011**, *17*, 3868.
- (11) Lenosky, T.; Gonze, X.; Teter, M.; Elser, V. *Nature* **1992**, *355*, 333.
- (12) Townsend, S. J.; Lenosky, T. J.; Muller, D. A.; Nichols, C. S.; Elser, V. *Phys. Rev. Lett.* **1992**, *69*, 921.
- (13) Bharat; Bhola, R.; Bally, T.; Valente, A.; Cyrański, M. K.; Dobrzycki, Ł.; Spain, S. M.; Rempala, P.; Chin, M. R.; King, B. T. *Angew. Chem., Int. Ed.* **2010**, *49*, 399.
- (14) Reisch, H. A.; Bratcher, M. S.; Scott, L. T. *Org. Lett.* **2000**, *2*, 1427.
- (15) Stabel, A.; Herwig, P.; Müllen, K.; Rabe, J. P. *Angew. Chem., Int. Ed. Engl.* **1995**, *34*, 1609.
- (16) Wu, J.; Pisula, W.; Müllen, K. *Chem. Rev.* **2007**, *107*, 718.
- (17) Xiao, S.; Myers, M.; Miao, Q.; Sanaur, S.; Pang, K.; Steigerwald, M.; Nuckolls, C. *Angew. Chem., Int. Ed.* **2005**, *44*, 7390.
- (18) Sakamoto, Y.; Suzuki, T. *J. Am. Chem. Soc.* **2013**, *135*, 14074.
- (19) (a) Miller, R. W.; Duncan, A. K.; Schneebeli, S. T.; Gray, D. L.; Whalley, A. C. *Chem. - Eur. J.* **2014**, *20*, 3705. (b) Miller, R. W.; Averill, S. E.; Van Wyck, S. J.; Whalley, A. C. *J. Org. Chem.* **2016**, *81*, 12001.
- (20) Our recent attempts to synthesize hepta-*peri*-heptabenzo-[7]circulene were not successful. See: Yang, X.; Miao, Q. *Synlett* **2016**, *27*, 2091.
- (21) Platt, K. L.; Oesch, F. *J. Org. Chem.* **1981**, *46*, 2601.
- (22) Desai, N. B.; McKelvie, N.; Ramirez, F. *J. Am. Chem. Soc.* **1962**, *84*, 1745.
- (23) Chiu, C.-Y.; Kim, B.; Gorodetsky, A. A.; Sattler, W.; Wei, S.; Sattler, A.; Steigerwald, M.; Nuckolls, C. *Chem. Sci.* **2011**, *2*, 1480.
- (24) Hatanaka, M. *J. Phys. Chem. A* **2016**, *120*, 1074.
- (25) Shen, M.; Ignatyev, I. S.; Xie, Y.; Schaefer, H. F. *J. Phys. Chem.* **1993**, *97*, 3212.
- (26) (a) Becke, A. D. *J. Chem. Phys.* **1993**, *98*, 5648. (b) Miehlich, B.; Savin, A.; Stoll, H.; Preuss, H. *Chem. Phys. Lett.* **1989**, *157*, 200. (c) Lee, C.; Yang, W.; Parr, R. G. *Phys. Rev. B: Condens. Matter Mater. Phys.* **1988**, *37*, 785.
- (27) Anslyn, E. V.; Dougherty, D. A. *Modern Physical Organic Chemistry*; University Science Books: Sausalito, CA, 2004; Chapter 7.
- (28) Feng, C.-N.; Hsu, W.-C.; Li, J.-Y.; Kuo, M.-Y.; Wu, Y.-T. *Chem. - Eur. J.* **2016**, *22*, 9198.
- (29) Laudise, R. A.; Kloc, C.; Simpkins, P. G.; Siegrist, T. *J. Cryst. Growth* **1998**, *187*, 449.
- (30) HOMO = -5.10 eV - E_{ox} (versus Fc⁺/Fc). See: Cardona, C. M.; Li, W.; Kaifer, A. E.; Stockdale, D.; Bazan, G. C. *Adv. Mater.* **2011**, *23*, 2367.
- (31) Xu, X.; Yao, Y.; Shan, B.; Gu, X.; Liu, D.; Liu, J.; Xu, J.; Zhao, N.; Hu, W.; Miao, Q. *Adv. Mater.* **2016**, *28*, 5276.
- (32) Liu, D.; He, Z.; Su, Y.; Diao, Y.; Mannsfeld, S. C. B.; Bao, Z.; Xu, J.; Miao, Q. *Adv. Mater.* **2014**, *26*, 7190.
- (33) Tremblay, N. J.; Gorodetsky, A. A.; Cox, M. P.; Schiros, T.; Kim, B.; Steiner, R.; Bullard, Z.; Sattler, A.; So, W.-Y.; Itoh, Y.; Toney, M. F.; Ogasawara, H.; Ramirez, A.; Kymissis, I.; Steigerwald, M. L.; Nuckolls, C. *ChemPhysChem* **2010**, *11*, 799.
- (34) Kang, S. J.; Kim, J. B.; Chiu, C.-Y.; Ahn, S.; Schiros, T.; Lee, S. S.; Yager, K. G.; Toney, M. F.; Loo, Y.-L.; Nuckolls, C. *Angew. Chem., Int. Ed.* **2012**, *51*, 8594.